Water Research 243 (2023) 120390

Contents lists available at ScienceDirect

Water Research

journal homepage: www.elsevier.com/locate/watres

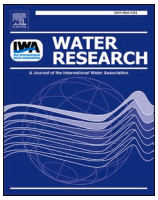

Mercury budgets in the suspended particulate matters of the Yangtze River

Dong Peng [a,b,#], Jixuan Lyu [b,#], Zhengcheng Song [a], Shaojian Huang [a], Peng Zhang [a], Jianhua Gao [b,*], Yanxu Zhang [a,c,*]

[a] Nanjing University, School of Atmospheric Sciences, 163 Xianlin Road, Qixia Distinct, Nanjing 210023, China
[b] Nanjing University, School of Geography and Ocean Science, Ministry of Education Key Laboratory for Coast and Island Development, 163 Xianlin Road, Qixia Distinct, Nanjing 210023, China
[c] Frontiers Science Center for Critical Earth Material Cycling, Nanjing University, Nanjing 210023, China

ARTICLE INFO

Keywords:
Dam effects
Mercury emission
Riverine mercury flux
Mercury sedimentation
Pandemic impact

ABSTRACT

Riverine processes are crucial for the biogeochemical cycle of mercury (Hg). The Yangtze River, the largest river in East Asia, discharges a substantial amount of Hg into the East China Sea. However, the influencing factors of the Hg budget and its recent trends remain unclear. This study quantitatively analyzed the total Hg concentration (THg) in suspended particulate matter (SPM) in the Yangtze River and calculated the Hg budget in 2018 and 2021. The results showed that the total Hg concentrations varied substantially along the river, with concentrations ranging from 23 to 883 μg/kg in 2018 and 47 to 146 μg/kg in 2021. The average Hg flux to China Sea in 2018 and 2021 were approximately 10 Mg/yr, lower than in 2016 (48 Mg/yr). Over 70% of the SPM was trapped in the Three Gorges Dam (TGD), and 22 Mg/yr of Hg settled in the TGD in 2018 and 10 Mg/yr in 2021. Hg fluxes in the Yangtze River watershed were driven by various factors, including decreased industrial emissions, increased agriculture emissions, and decreased soil erosion flux. We found that in the upper reach of the Yangtze River changed from sink to source of Hg possibly due to the resuspension of sediments, which implies that the settled sediments could be a potential source of Hg for downstream. Overall, emission control policies may have had a positive impact on reducing Hg flux to the East China Sea from 2016 to 2021, but more efforts are needed to further reduce Hg emissions.

1. Introduction

Mercury (Hg) is a neurotoxin that has emerged as a significant environmental issue worldwide due to the rapid development of industry and the economy. Hg compounds can be found in land, ocean, and atmosphere, and are transported through a biogeochemical cycle with various forms (Boening 2000; Driscoll et al., 2013). Rivers serve as a vital link between land and ocean in the Hg cycle, allowing for the transport of Hg from land to ocean (Amos et al., 2014; Gao et al., 2017; Liu et al., 2021). The Hg budget in the global rivers, however, has been under-studied in previous research, while the increasing complexity of river systems resulting from the construction of numerous reservoirs and dams in recent decades (Selin et al., 2008; Liu et al., 2019).

The Hg budgets of rivers are primarily controlled by the concentration of Hg in suspended particulate matter (SPM) and the sediment flux, given that most riverine Hg is contained in SPM (Cranston and Buckley, 2002; Liu et al., 2021). Industrial emissions are a major contributor to the riverine Hg (Pacyna et al., 2006; Kocman et al., 2017; Muntean et al., 2018). Specifically, iron and steel production, Artisanal and Small-Scale Gold Mining (ASGM) are listed as the important sources of Hg emissions (Pang et al., 2022) and caused relatively high Hg contributions to river systems (Kocman et al., 2017). Natural sources, especially soil erosion, are also important contributors, mainly affected by land use, precipitation, and soil properties. Other human activities, such as land use changes and reservoir construction, also have a significant and increasing impact on Hg riverine budgets.

Previous studies have investigated the Hg budget in a few rivers from different regions. Liu et al. (2021) reported the Hg budgets of major rivers in East Asia, including the Yangtze River, Yellow River, Pearl River, and Rivers-Japan. These rivers were found to be the major contributors of Hg into the East China Sea with budget ranges from 0.07 Mg/yr to 48 Mg/yr, surpassing the contribution of atmospheric deposition. The study also revealed a strong correlation between Hg and SPM in these rivers. Buck et al. (2015) studied the Hg budget in rivers leading

* Corresponding authors.
E-mail addresses: jhgao@nju.edu.cn (J. Gao), zhangyx@nju.edu.cn (Y. Zhang).
# The author has equal contribution to this research.

https://doi.org/10.1016/j.watres.2023.120390
Received 31 May 2023; Received in revised form 16 July 2023; Accepted 19 July 2023
Available online 22 July 2023
0043-1354/© 2023 Elsevier Ltd. All rights reserved.

to northern Gulf of Mexico estuaries in the US. They found that the Mississippi River had the highest Hg budget of 0.62 Mg/yr, contributing 59% of the total Hg flux into the estuaries of the northern Gulf of Mexico. The study suggests that rivers are significant sources of Hg in the Gulf of Mexico, while estuaries act as sinks for Hg. Global riverine Hg discharge inventories were also developed in previous studies. The estimates of Arctic rivers' output 37 Mg Hg to the Arctic Ocean per year were based on records of six major rivers (Zolkos et al., 2020). Amos et al. (2014) reported that approximately 5500 Mg/yr of Hg flux was discharged by rivers globally into the ocean. Recently, Liu et al. (2021) considered the temporal and spatial variations in the global estuaries and updated the estimate to suggest that about 1000 Mg of Hg is delivered annually from global rivers to the ocean.

The Yangtze River watershed, the largest in East Asia, has a considerable contribution to sediment and Hg transport to the East China Sea. The Yangtze River is home to several mega-cities and dams, located in the temperate monsoon zone, and is, therefore, an ideal location for studying the impacts of anthropogenic and climate changes on river systems. Previous studies on the Yangtze River have found significant interannual variability in the Hg budget. For example, Liu et al. (2020a) reported that up to 110 Mg Hg had been delivered to the East China Sea by the Yangtze River in 2014–2015, but 48 Mg Hg in 2016 (Liu et al., 2021). The exact reason for this variability remains unclear but two main factors may contribute: (1) implementation of Hg and other pollutant emission control policies (Mulvaney et al., 2020); and (2) water management practices like dams and reservoirs that impact the sediment budget (Gao et al., 2018). In addition, the Minamata Convention that took effect in 2017 and the recent COVID-19 lockdown, may also influence the source-sink pattern of tributaries and mainstream in the Yangtze watershed.

In this study, we collected samples along the Yangtze River, covering approximately 3500 km of the river in 2018 and two seasons in 2021. We aimed to evaluate the riverine Hg fluxes in SPM in the Yangtze River watershed and the output fluxes to the East China Sea in 2018, July 2021, and Oct. 2021. We compared them with those in previous years and evaluated their association with emission data sets and natural environment factors to identify the key factors that impact the Hg flux in the Yangtze River. Additionally, we analyzed the connection between Hg and carbon/nitrogen compounds in SPM and discussed the effects of the Three George Dam and mega-cities on the Hg budget in the Yangtze River.

2. Materials and methods

2.1. Sample collecting

Field sampling was conducted in the Yangtze River watershed in August 2018, July 2021, and October 2021. The location of the Yangtze River Watershed is presented in Fig. 1**a**. The surface water samples (0–1 m) were collected by using an acid-washed polyethylene sampler in the mainstream of the river channel, as well as in the tributaries (eleven samples in the mainstream and nine samples in tributaries, Fig. 1**a**). The SPM was obtained by filtration: the water samples were filtered by 0.7 μm glass fiber filters (47 mm diameter, Whatman GF/F) which had been

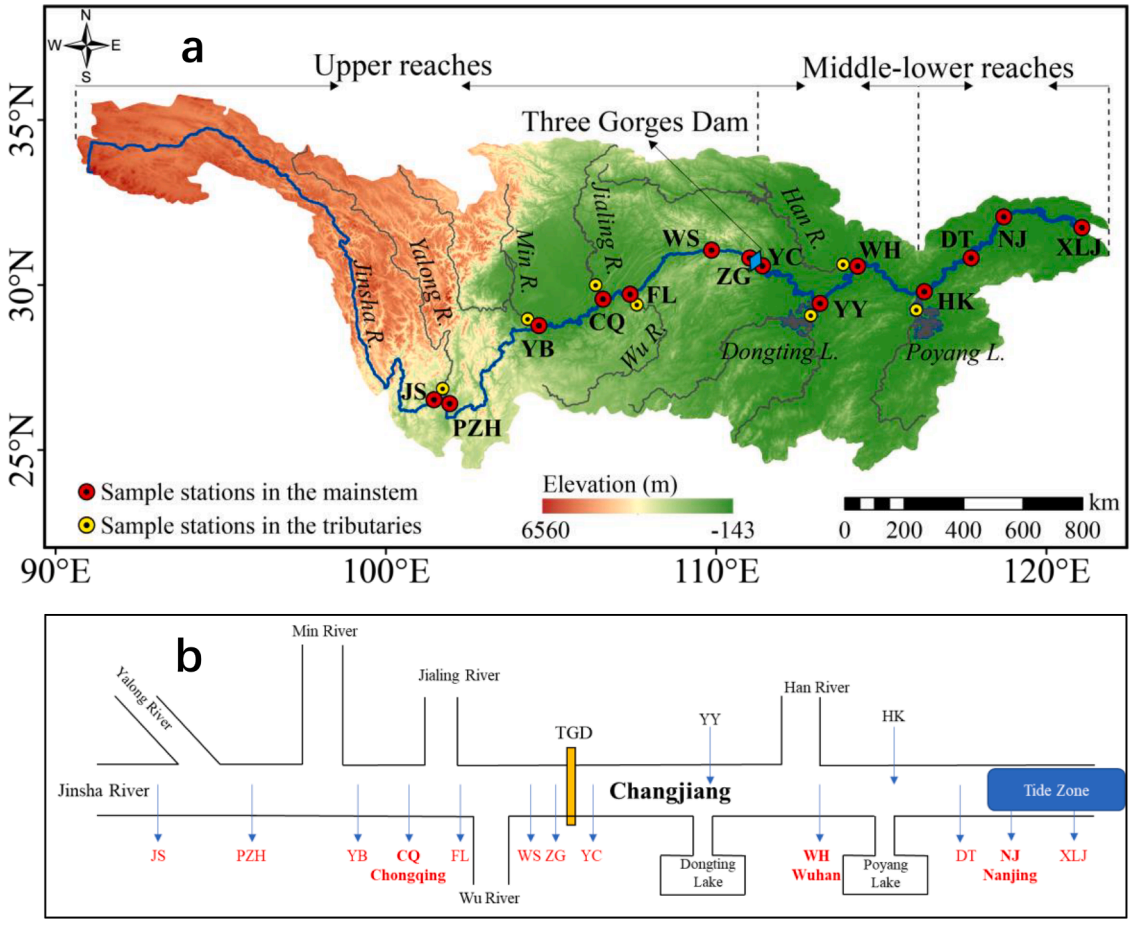

Fig. 1. a) Location of the Yangtze River in China and sample sites in the Yangtze River Watershed; b) concept map of the Yangtze River Watershed, the dark yellow bar represents the dam (Three Gorges Dam, TGD), the flow in channels represents tributaries rivers, the boxes represent tributaries lakes, the red capital notes represent the sample sites, and the bold red text represents mega-cities. The detail of sample site (acronyms) was given in **Table A.2-Appendix A**. (For interpretation of the references to colour in this figure legend, the reader is referred to the web version of this article.)

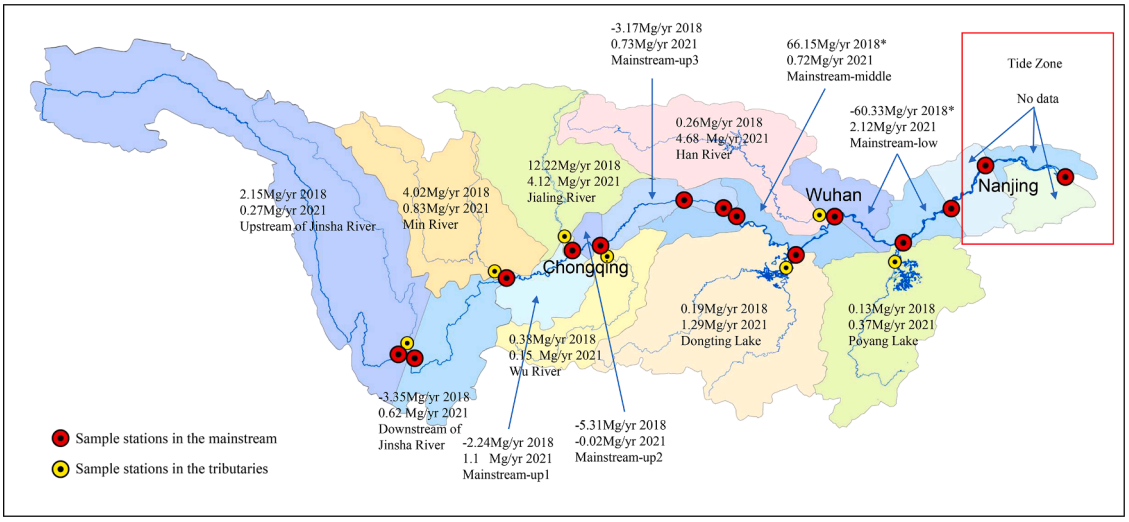

Fig. 2. The observed net mercury flux of the sub-watershed. The numbers represent the net mercury flux of the sub-watershed (Mg/yr) in 2018 or 2021. The Mainstream-up1–3 represents the sub-watershed in the upper reach of the Yangtze River and ranks as 1–3 along the flow direction, the Mainstream-middle/low represents the middle/lower reaches. The asterisk remarks indicate that the data were influenced by abnormal values (explained in the result), the tide zone represents the zone that could be influenced by tide for which there are no net mercury flux data. The Chongqing, Wuhan and Nanjing are mega-cities.

pre-combusted at 450 °C for 3 h for cleaning, and pre-weighed (Buck et al., 2015). The filtered matter (SPM) was frozen dried and then stored at −20 °C for further laboratory analysis.

2.2. Lab analysis

All SPM samples were stored in PE bags and refrigerated at −20°C. The total Hg concentration of samples was determined by Mercury Test (DMA-80, Milestone, Italy). The test processes were: firstly, the Standard sediment [GBW07405(GSS-5), solid, Institute of Geophysical and Geochemical Exploration, Hg 290 mg/kg; GBW07423(GSS-9), solid, Institute of Geophysical and Geochemical Exploration, Hg 30 mg/kg] were used to calibrate the instrument; next, we analyzed the samples in triplicate; then any sample that was considered as outlier [by Dixon's Q-test (Efstathiou 2006)] were retested; finally, we record all data and remove the outlier before statistics. There were 53 samples in total, and 47 of them were tested with more than three replicates. Six samples were tested twice because they do not have enough materials for the third test. The maximum accepted coefficient of variation (RSD) was 12.5%. The R square of the calibration curve was >0.999.

2.3. Data sets

In this study, we cited several data sets to figure out what were the major causes for the unique Hg budgets in the Yangtze River. The global atmospheric mercury emission inventory (EDGAR, 2012,) was chosen as a proxy for the Hg release to the freshwater environment due to its data availability. Indeed, Hg release to the atmosphere and freshwater environment arises from major industrial source sectors, e.g., chlor-alkali industry, oil refining, gold, and non-ferrous metal production, and disposal of Hg-containing products (Kocman et al., 2017). Also, the human activity data sets like GDP (2010) (XU Xinliang 2014), and population (2010) (Shen et al., 2017) in China were also chosen to scale the Hg emission strength. Other data sets related to natural Hg sources like land use (2020, GlobeLand 30, (Jun et al., 2014; Chen et al., 2017)), Slope (SRTMSLOPE 90 M), Precipitation (2018, 2021) (Peng et al., 2019; Ding and Peng, 2020) and soil parameters (Shangguan et al., 2013) were also considered for the correlation analysis with our data (See **Appendix A** for more detail). The population, GDP, precipitation and soil parameters were regional data sets and other data sets were at global scale. All data sets were in grid format and the regional/watershed values were extracted using the Yangtze River Watershed vector map.

2.4. Statistics

We used the annual sediment fluxes published by China government to estimate the particulate Hg fluxes of the Yangtze River watershed:

$$Hg_f = Hg_c \times Sed_f \quad (1)$$

Hg_f represents the total Hg flux of each sub-watershed; Hg_c represents the Hg concentration of the monitor station sites of each sub-watershed. Note that Hg concentrations in the wet season were used because of the major contribution of sediment. Sed_f represents the total sediment flux of sub-watershed of the year (MWR 2016; MWR 2018; MWR 2021). The particulate Hg was the major part (>70%) of the riverine Hg (Cranston and Buckley, 2002; Liu et al., 2021), thus we use particulate Hg flux to represent the Hg flux of the rivers.

We calculated Hg fluxes at the hydrology monitor stations [the detail of stations can be found in (MWR 2016; MWR 2018; MWR 2021)] and sampling sites (Fig. 1**a, b**) along the Yangtze River. These fluxes were compared with the natural and socio-economical parameters of corresponding sub-watersheds that potentially contribute to these sampling sites (Fig. 2). We considered 17 sub-watersheds with all parameter data sets clipped by the boundary of watersheds by ArcGIS Pro 2.8.3 (ESRI. Redlands, CA: Environmental Systems Research Institute). Except for tributaries that are naturally divided into different watersheds, the Jinsha River was separated into two parts by Guanyinyan Reservoir, and the mainstream of Yangtze River was divided into several sub-watersheds defined by the contribution to the monitoring stations (Fig. 1**a**, upper and middle-lower reaches). The extension data like GDP were summarized as the sum of the sub-watershed and status data like soil pH were summarized as the average of the sub-watershed. Spearman Correlations, pairwise analysis, and Linear fit were applied to the Yangtze River Hg flux and summarized data set by JMP Pro 16 (SAS Institute Inc., Cary, NC, 1989–2021).

3. Results and discussion

3.1. Temporal and Spatial distribution of Hg concentration and Hg flux in the Yangtze River

Concentration of the total Hg (THg) and its fluxes in the Yangtze River were portrayed in graphical form in Fig. 3 and Fig. 4. The national background level of Hg is 150 μg/kg (Zhang et al., 2018). Fig. 3 shows the THg concentrations along the mainstream Yangtze River, which ranged from 23.46±3.14 to 882.97±4.06 μg/kg in 2018, 47.28±0.37 to 103.92±6.80 μg/kg in July 2021, and 48.95±1.71 to 146.14±5.87 μg/kg in October 2021. The concentration of THg in the Yangtze River watershed is similar to previous records found in developing regions such as the Awash River in Ethiopia [170 μg/kg, (Dirbaba et al., 2018)] and the Yangtze River in 2016 [210±56 μg/kg, (Liu et al., 2020b)]. It is higher than that found in the less polluted rivers like the Esaro River in Italy [44 μg/kg, (Protano et al., 2014)], but lower than that found in high-emission areas such as Candarli Gulf, Turkey [230–1400 μg/kg, (Pazi 2011)], highly industrialized regions like Hyeongsan River, South Korea [0.11–35.6 mg/kg, (Bailon et al., 2018)], mine areas like Tisza, Hungary [330–770 μg/kg, (Devai et al., 2007)], Gulf of Trieste [Slovenia, Idrija mining, 610–6870 μg/kg, (Pavoni et al., 2023)], Paglia–Tiber River [Italy, Monte Amiata mining, 1.53–288.57 μg/g (= particulate Hg/ total suspended solid), (Fornasaro et al., 2022)] and Shuangqiao River [China; Xiaoqinglin gold area; 0.8–1.12 mg/kg, (Liu et al., 2012)].

The Hg flux exhibited a different pattern compared to the THg concentration due to the varied sediment fluxes in the Yangtze River watershed. Fig. 4 shows the flux of THg in SPM at the different sampling sites. The Hg budget of the Yangtze River into the East China Sea was approximately 10 Mg/yr in 2018 and 2021, much lower than a previous study that reported a flux of 48 Mg/yr (dissolved Hg + particulate Hg) output from the Yangtze River to the East China Sea in 2016 (Liu et al., 2020b). The output Hg flux in the Yangtze River was similar to the Yellow River (China, 9.9 Mg/yr, (Liu et al., 2021)), and Pearl River (China, 9.7 Mg/yr, (Liu et al., 2021)), even though the Yangtze River has much higher sediment flux than the other two rivers. However, we found much higher flux in the Yangtze River than in the Mississippi River (U.S., 0.62 Mg/yr, (Buck et al., 2015)), likely due to the lower sediment flux of the latter and low industry activity in the watershed. In contrast, the output Hg flux of the Yangtze River is lower than Mekong River (East Asia, 21 Mg/yr, (Noh et al., 2013)), likely attributable to the less strict wastewater management in the watershed of the latter river (Creaser et al., 2019).

The data in 2021 included two seasons: wet (July) and dry (October). In general, there were no significant differences in THg concentration between the wet season (July) and dry season (October) of 2021 (Fig. 3), despite more soil could enter the river system during flooding events in the wet season. The Hg concentration in SPM was likely controlled by the Hg concentrations in erosional soil, rather than the dissolved Hg (II) bonding into SPM in the river because the flow flux has less impacts on THg concentration.

Cities usually act as the major sources of Hg because of industrial emissions. The mega-cities (Chongqing, Wuhan, Nanjing) in the Yangtze River were marked in Fig. 1**b**. The sampling records around mega-cities in the Yangtze River watershed showed similar THg concentration levels, regardless of their locations in upstream, midstream, or downstream of the river (Fig. 1**b,** Fig. 2**b**). However, Wuhan had an abnormal highest THg concentration in August 2018, possibly due to an instantaneous emission event during sampling. Possible source(s) for such specific event could be represented by shipping activities, coal combustion, and iron industries in Wuhan, a major industrial city in central China (Yi et al., 2011; Sun et al., 2013).

The tributaries contribute substantially to the Hg in the Yangtze River. The THg concentrations of the tributaries of the Yangtze River ranged from 35.78±2.73 (Yalong River) to 168.01±5.85 μg/kg (Jialing River) in 2018, and 65.17±2.36 (Yalong River) to 115.52±2.99 μg/kg (Dongting Lake) in July 2021. Approximately 20 Mg Hg were discharged from tributaries into the Yangtze River in 2018 and almost 10 Mg in 2021. The Hg flux of the tributaries ranged from 0.19 (Dongting Lake) to 12.22 Mg/yr (Jialing River) in 2018 and ranged from 0.15 (Wu River) to 4.12 Mg/yr (Jialing River) in 2021 (Fig. 3**b**). Jialing River and Min River have the largest contributions to THg flux among tributaries (Fig. 3**b**). The Hg flux was found to be higher in Chongqing (CQ, Fig. 4**a**) compared to downstream of the Jialing River confluence (referred to as FL, Fig. 4**a**). Interestingly, although the Jialing River contributed a substantial Hg flux to the mainstream downstream of CQ, the presence of the Three Gorges Reservoir in the FL area led to lower flow speeds, resulting in increased sedimentation and reduction of Hg flux. This phenomenon likely contributed to the higher Hg flux observed in Chongqing.

3.2. Driving factors of sub-watershed variations

The watershed of the Yangtze River has been divided into as 17 subwatersheds for analysis (Fig. 2). Correlation analysis (Pairwise analysis and Spearman analysis) was conducted between the net mercury flux (nMF, the upstream Hg flux subtracted from the downstream Hg flux, i.e., the new contribution from the corresponding watershed) of 14 subwatersheds (two of 17 were combined into one and three had no data) and potential influencing factors (see Fig. 2 for nMF). These factors were classified as emission data sets and erosion data sets by their potential impacts on Hg fluxes. The emission data sets include atmospheric Hg emission sources (EDGAR), population, and GDP. The erosion data sets represent Hg flux by soil erosion and subsequent sediment fluxes. The erosion data sets included land use, the slope of the land, precipitation, and soil properties (Table 1). As many factors of the data sets have different ranges and distribution types, we uniformed them by using either Z score or Logarithm-based transformation. All significant correlations are given in Table 2 and discussed below.

The nMF in 2018 and 2021 both had a significant correlation with EDGAR ($p<0.05$, Table 2), especially iron and steel production (iro). This is attributed to the prosperity of iron steel industries and auto manufacturing along the Yangtze River (Sun et al., 2013; Han et al., 2019; Gao and Xing, 2021), particularly in Chongqing, Wuhan, and Shiyan, and which were also associated with other pollutions like air pollution (Mao et al., 2013). Iron ore materials contain Hg, which is emitted during steel production processes. Six sectors of EDGAR had significant correlation with nMF in 2018 by pairwise correlation (Table 2, $p<0.05$) while only two sectors of EDGAR were significantly correlated with nMF in 2021. The weaker linear correlation between nMF and emission factors in 2021 compared to 2018 was caused by the reduction of industrial Hg emissions during this period, which were caused by the mutual effects of lockdown (pandemic of COVID19) and stricter emission control policies of Hg after Minamata Convention (Mulvaney et al., 2020; Shen et al., 2021). Based on Spearman analysis, the nMF in July 2021 was substantially influenced by six sectors of EDGAR (Spearman, $p<0.05$). The population had an impact on nMF in July 2021 ($p<0.05$), but GDP had less significance with nMF, related to the lockdown policy during pandemic. Strict pandemic policies in China resulted in reduced human mobility during this period (Kraemer et al., 2020). In 2021, the increased utilization of medical resources resulting from the pandemic led to an increase in improper disposal of medical waste; this includes incineration and landfill of such waste in areas that lack adequate capacity for its management (Sangkham 2020), the latter would result in Hg release to ecosystems (Lee et al., 2016; Peng et al., 2021) and the Hg emission from landfilled-waste was reported in Wuhan (Sun et al., 2013).

In aquatic ecosystems, 80% of Hg compounds in water are bound with SPM (Schuster et al., 2011; Amos et al., 2014) therefore soil erosion should be highlighted as another factor to be considered. Prior study indicated that soil erosion is another important contributor to the Hg in

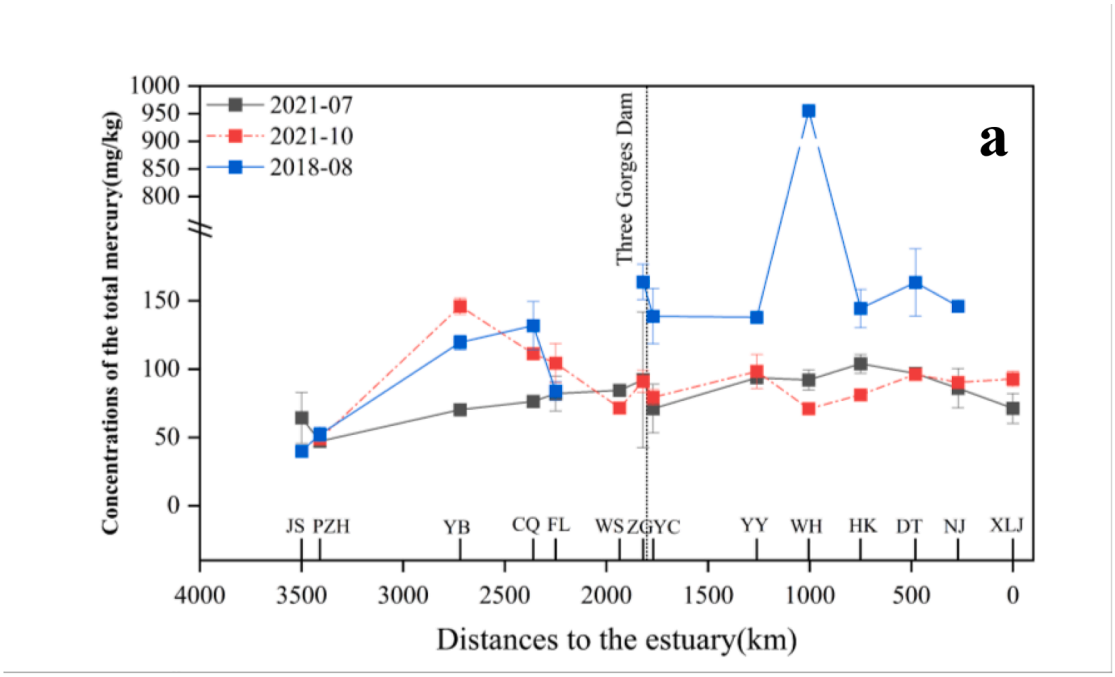

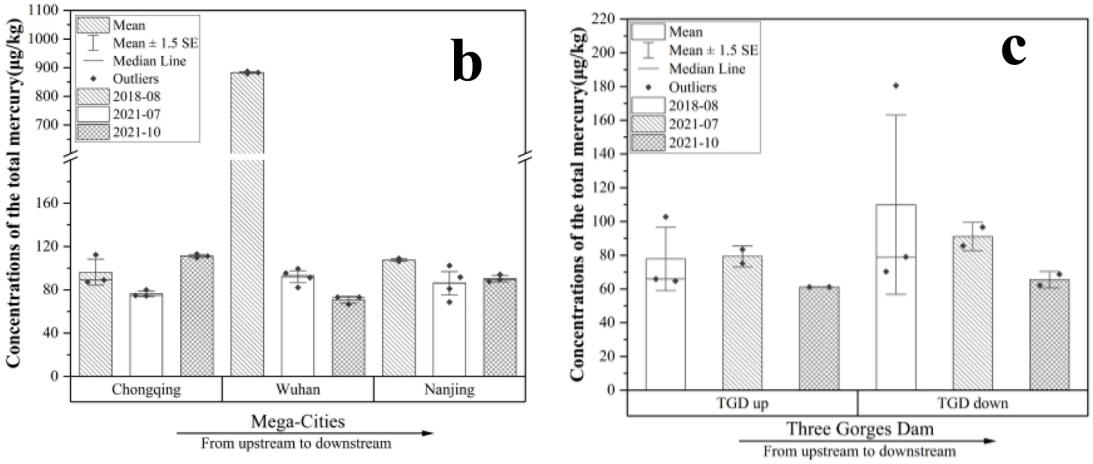

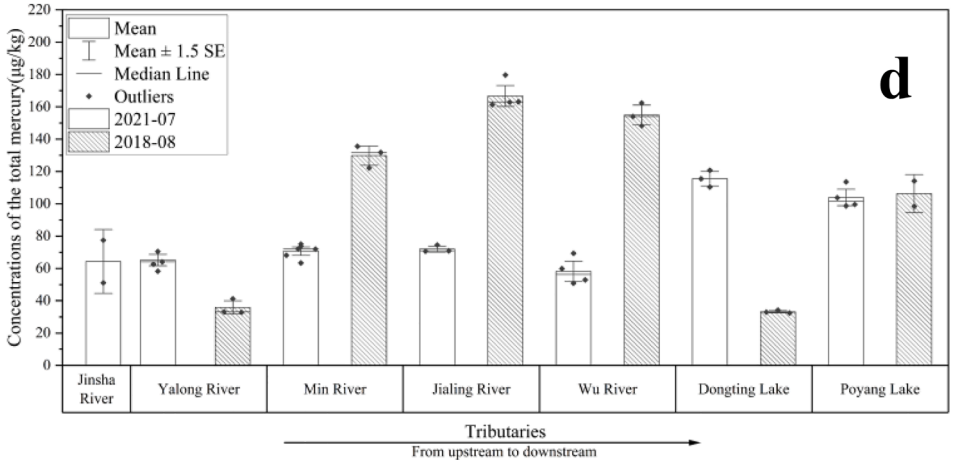

Fig. 3. Concentration of total mercury in suspended particulate matter of Yangtze River in 2018 and 2021. a) concentration of total mercury in mainstream of Yangtze River; b) concentration of total mercury in mega-cities of Yangtze River; c) concentration of total mercury in upstream and downstream of Three George Dam (TGD); d) concentration of total mercury in tributaries of Yangtze River watershed.

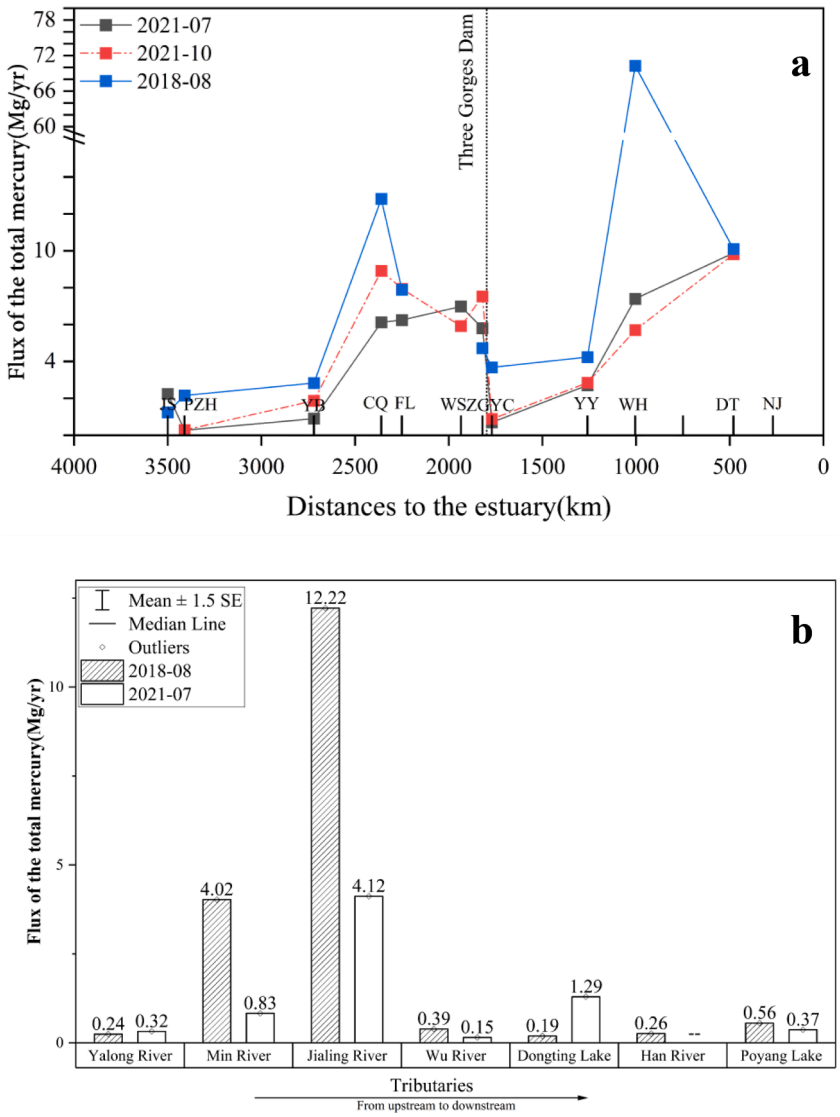

Fig. 4. Fluxes of total mercury in suspended particulate matter of Yangtze River in 2018 and 2021. a) flux of total mercury in the mainstream of the Yangtze River; b) contribution of the total mercury flux from tributaries to the Yangtze River.

Table 1
The classification of data sets.

Data sets	Data sets	Description
Emission Data sets	EDGAR	Atmosphere Emission
	Population	Anthropogenic sources
	GDP	Anthropogenic sources
Erosion Data sets	Landuse-GlobeLand 30	Land Use data
	Soil parameters	Soil properties data
	Slope	Geography slope data
	Precipitation	Monthly precipitation data

the Yangtze River (Liu et al., 2020b), so we evaluated the association between Hg flux and erosion data sets parameters. Soil erosion fluxes are influenced by soil properties such as grain size, driving factors like precipitation, and geographic factors such as land slope. We find the variables of land use and soil properties were correlated with nMFs (Table 2). The cropland and wetland had positive correlations with nMF. The wet cropland acts as the sink of atmospheric Hg (Wang et al., 2016) and is likely to be the source of soil erosion (Guerra et al., 2017). The wetland showed stronger correlation with the nMF in 2021, which were caused by the fishery industry sources of Hg (Peng et al., 2020). Specifically, the policy of the ten-year ban on fishing in the Yangtze River from 2021 to 2031 led to the rise of fish farming, which made wetlands become important sources of pollutants (XU 2021). The land use types of bare and glacial had negative correlations with nMF in July 2021, possibly because these land types are uncovered by vegetation. As a consequence, there is either causing either a less atmospheric deposition flux to soil or a higher Hg release flux from soil to atmosphere, or both (Ma et al., 2018), and consequently a lower Hg content in the surface layer. While the erosion fluxes from bare and glacial land are generally larger compared to other land types, the corresponding Hg fluxes remain relatively low.

The soil parameters in different layers of soil had various effects on nMF. The soil dominant structure (S1_1st-6th) had a positive correlation with nMF in the first layer but negative in the third layer (Table 2, $p<0.05$). The soil root abundance (R_1st-6th) had a positive correlation with nMF in the deeper layer (Table 2, $p<0.05$). A denser root presence increases the porosity of the soil, it helps to transfer Hg from the soil to the sub-river. The colors of the soil (with unclear water conditions, Unh_1st-6th; and wet color, Wh_1st-6th) were identified as significant factors affecting nMF in 2021. The red soil corresponded to higher nMF and the red-purple soil corresponded to lower nMF. Possibly, the red soil (rich in Fe^{3+}) impacts on nMF (Ma et al., 2014) and the impacts

Table 2
Correlation Analysis of mercury flux with parameters. log10, log, and Z represent the data centralization methods, 1st −6th represents the layers of soil, S1 represent soil dominant structure, U represents soil color (water condition unclear), Wh represents soil wet color, R represents root abundance factor, waste (solid waste incineration and agricultural waste burning), tro (road transport), iro (iron and steel production), glass (glass production), comb_res (combustion in residential and other combustion (transformation industry and oil refineries)), comb_power (combustion in power generation and in industry), cement (cement production) represent sector of EDGAR. Ranks of soil color parameters and root abundance factor are given in **Appendix A**.

Pairwise Analysis Variable	By Variables	Variable Data sets	Prob > |ρ|	Positive or Negative
Log10 (MF21_07)	Log10[S1_1st]	Erosion	0.02	P
	Log10[S1_3rd]	Data sets	0.04	N
	Log10[Unh_3rd]		0.04	–
	Log10[R_5th]		0.02	P
	Log10[Unh_5th]		<0.05	–
	Log10[wetland]		0.02	P
	Log10[bare]		0.02	N
	Log10[cropland]		0.04	P
	Log10[glacial]		0.01	N
	Log10[tro]	Emission	0.04	P
	Log10[iro]	Data sets	0.01	P
Log10 (MF21_10+1)	Log10[Unh_3rd]	Erosion	0.03	–
	Log10[Wh_3rd]	Data sets	<0.05	–
	Log10[Wh_4th]		0.04	–
	Log10[Unh_5th]		0.03	–
	Log10[Wh_5th]		0.04	–
	Log10[wetland]		0.01	P
	Log10[iro]	Emission	<0.05	P
	Log10[nfe_oth]	Data sets	0.01	P
Z(MF18)	Z[cropland]	Erosion Data sets	0.02	P
	Z[population]	Emission	0.04	P
	Z[waste]	Data sets	0.01	P
	Z[tro]		0.01	P
	Z[iro]		0.03	P
	Z[glass]		0.02	P
	Z[comb_power]		0.04	P
	Z[comb_res]		<0.05	P
	Z[cement]		0.01	P

Spearman Analysis Variable	By Variables	Variable Data sets	Prob > |ρ|	Positive or Negative
Log10(MF21_07)	Log10(S1_1st)	Erosion	0.03	P
	Log10(S1_4th)	Data sets	0.04	N
	Log10(R_6th)		0.02	P
	Log10(cropland)		0.02	P
	Log10(bare)		0.03	N
	Log10(population)	Emission	<0.05	P
	Log10(waste)	Data sets	0.02	P
	Log10(tro)		0.03	P
	Log10(iro)		0.03	P
	Log10(glass)		0.02	P
	Log10(comb_res)		0.04	P
	Log10(cment)		<0.01	P
Log10(MF21_10+1)	Log10(waste)	Emission	0.03	P
	Log10(comb_res)	Data sets	0.03	P
	Log10(cment)		0.01	P
	Log10(cropland)	Erosion Data sets	<0.05	P
Z(MF18)	Z(CA_1st-CA_6th)	Erosion	<0.05	P
	Z(CEC_1st-CEC_5th)	Data sets	<0.05	P
	Z(GRAV_1st-GRAV_6th)		<0.05	P
	Z (MG_1st-MG_6th)		<0.05	P
	Z (POR_6th)		0.01	P
	Z(waste)	Emission	0.02	P
	Z(tro)	Data sets	0.03	P
	Z(iro)		0.04	P

consisted with increased agriculture emissions (in 2021). On the other hand, slope and precipitation did not show significant correlation with nMF which could be explained by (1) an average soil slope across the whole (sub-)watershed cannot represent the overall mobility potential of soil particles (Guerra et al., 2017), (2) not all precipitation drives erosion events (Owen et al., 2011; Guerra et al., 2017). Extreme hydrological events, such as rainstorms, play a crucial role in driving soil erosion (Dadson et al., 2003; Yin et al., 2023), while the type of vegetation cover acts as a significant protective factor in reducing soil erosion across various slopes (El Kateb et al. 2013). Indeed, a higher spatial resolution and mechanism-based model are needed to better reveal the impact of these factors.

We also examined the relationship between THg concentrations and the fractions of carbon and nitrogen in SPM in the Yangtze River watershed. The carbon and nitrogen data were obtained from Jixuan Lyu's previous studies on the Yangtze River watershed which were sampled together with this study (Wang et al., 2022; Lyu et al., 2023). The Hg-carbon relationship had been widely investigated in the rainfall (Akerblom et al., 2015), lakes (Driscoll et al., 1995), and wetlands (Kolka et al., 1999). However, a noteworthy inverse relationship was

Table 3
Correlation analysis between the total mercury concentrations with carbon and nitrogen percentage in particle matters of Yangtze River.

Time	By Variables	Method	Correlation	Signif Prob
2018	C%	Pairwise	−0.15	0.86
2018	N%	Pairwise	−0.04	0.51
2018	C%	Spearman	−0.59	<0.01**
2018	N%	Spearman	0.04	0.86
July 2021	C%	Pairwise	0.21	0.40
July 2021	N%	Pairwise	0.24	0.33
July 2021	C%	Spearman	−0.05	0.84
July 2021	N%	Spearman	−0.02	0.93

observed in 2018 between the concentration of carbon and THg (Table 3, $p<0.01$), whereas no correlation was found in 2021. This indicates that the carbon and Hg in SPM may have different sources: the former is from biological production in the river water while the latter is from soil erosion, wastewater discharge, and/or atmospheric deposition. Meanwhile, the nitrogen fractions also showed no correlation with THg concentrations. It could be the result of the lower abundance of plankton found in the Yangtze River than in previous studies. Specifically, the strong correlation between Hg and organic matters was usually found in wetlands (Kolka et al., 1999) and estuaries (Ramalhosa et al., 2005). However, the SPM in river channels usually had higher flow speed and fewer nutrient concentrations than in wetlands/estuaries, which could lead to less plankton development (He et al., 2017) and therefore smaller impacts on THg in SPM.

3.3. Decline of Hg in the Yangtze River

Fig. 5**b** illustrates the Hg budget of the mainstream of the Yangtze River into the East China Sea. The Hg fluxes showed different patterns from 2016, 2018, and 2021. Firstly, the Hg fluxes discharged to the ocean were steady in 2018 and 2021 (Fig. 4), which was caused by a compensation of the higher sediment flux and lower Hg concentration in the outlet of the Yangtze River to the ocean in 2018 compared to 2021. Compared with the previous study in 2016 (Liu et al., 2020b), the Hg budgets from the Yangtze River to the ocean were much lower in 2018 and 2021. Although there were only slight changes in the river's water flux from 2016 to 2021, a significant reduction was observed in sediment flux (Fig. 5**c**), likely caused by the construction of reservoirs along the river (Gao et al., 2017; Gao et al., 2018) and the increase in vegetation cover (Ananda and Herath, 2003; Liu et al., 2011). As we discussed before, erosion events and sediment flux were important factors that impact Hg flux. Therefore, it is reasonable that the different patterns of Hg flux in years could be associated with the different sediment flux in 2016, 2018, and 2021.

The Hg fluxes of the tributaries also differ substantially in 2018 and 2021 (Fig. 2). For example, the nMF of upstream of Jinsha River, Min River, Jialing River, and Wu River sub-watersheds had experienced a decline, which could be attributed to China's more stringent emission policies and soil erosion control policies. The Hg flux decreased by more than 60% in Jialing River and by 80% in Min River from 2018 to 2021, both of these tributaries contributed high Hg flux to mainstream. However, the low Hg fluxes sub-watersheds, such as Dongting Lake had observed a 6-fold increase in Hg flux and a 3-folder increase in Poyang

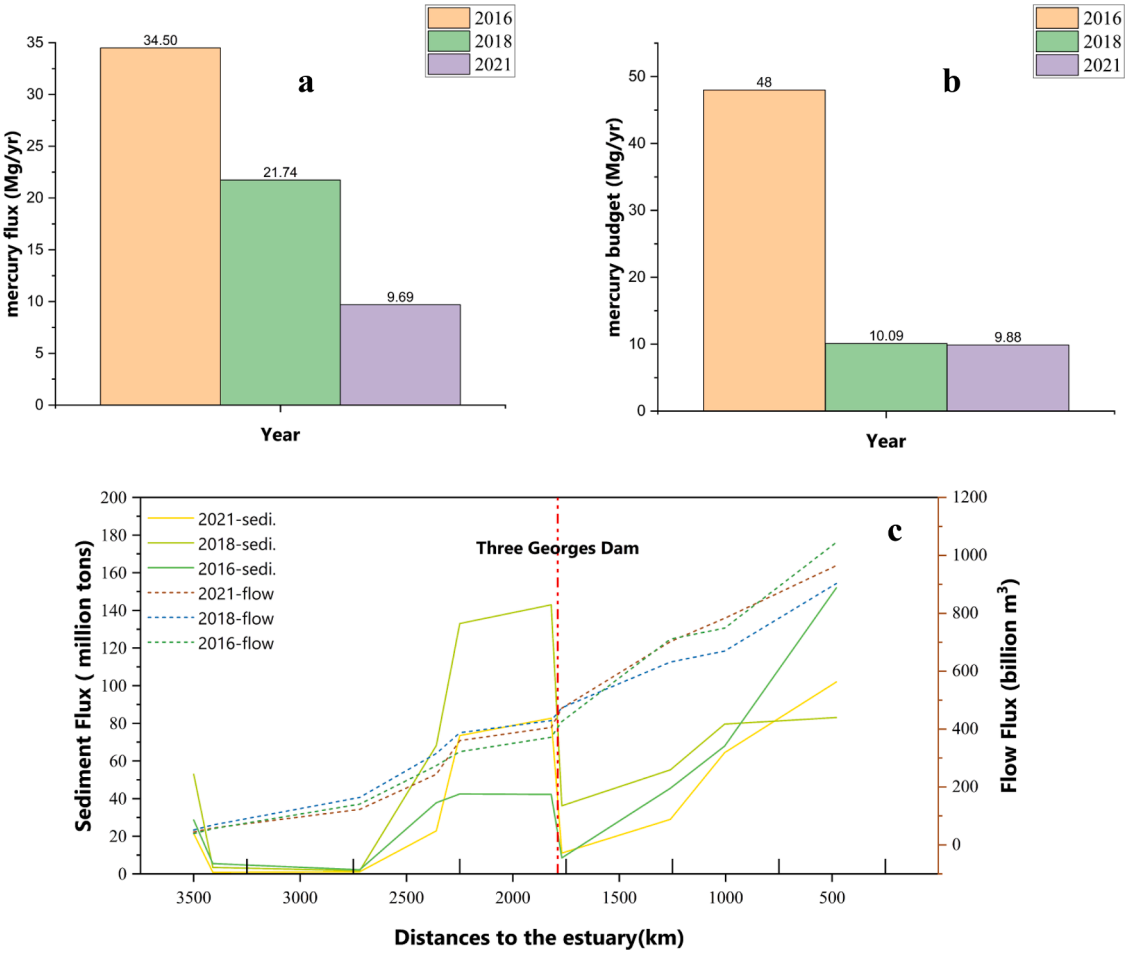

Fig. 5. **a**) Mercury flux settled in the TGD reservoir; b) mercury budgets of the Yangtze River [only the 2016 fluxes are those calculated by Liu et al. (2020b)] to the East China Sea; c) sediment fluxes and flow flux of Yangtze River to China Sea (Lee et al., 2016; Kraemer et al., 2020; Peng et al., 2021).

Lake. The rise in nMF of a few sub-watersheds may be the unintended consequence of the prosperity in certain areas of China (Peng et al., 2020; Peng et al., 2023) and its bad impacts on water quality were also recognized in previous studies (Feng et al., 2021). Besides the pandemic lockdown policies, high-polluting factories in China have been relocated from developed regions to developing ones due to the stricter regulation, which resulted in a relocation of Hg releases to freshwaters (Li et al., 2021; Shao et al., 2021).

These changes highlight the impact of related policies on Hg emissions. There could be a reduction of anthropogenic emissions from 2018 to 2021, especially as a result of the COVID-19 lockdown and industrial/residential wastewater control by mega-cities (Hu et al., 2021). This could be proven by the weak correlation between EDGAR and Hg fluxes of sub-watersheds in 2021. As we discussed before, the significant decrease in sediment flux exemplifies the success in mitigating erosion-related origins of Hg. Remarkably, agricultural sources have emerged as a significant contributor to the Hg flux, calling for more attention and control measures in this sector. Similarly, the uncontrolled industrial emissions in fast-developing regions are also hot-spots of Hg pollution.

3.4. The Three Georges Dam's impacts on Hg in the Yangtze River watershed

The Yangtze River is divided into upper and middle-lower reaches by the Three Georges Dam (TGD), which acts as a barrier to sediments. The upper reach brings sediments to TGD and most of them are settled before the dam. Previous studies reported that up to 98% of SPM can be trapped by TGD (Yang et al., 2014; Liu et al., 2020b). The settled Hg flux in TGD was calculated by the gross inlet flux of Hg (Hg flux in CQ plus Hg flux of Jialing River plus Hg flux of Wu River) subtract from the outlet flux of Hg (Hg flux in YC). We found ~10 Mg Hg was settled in TGD in 2021 and ~22 Mg in 2018 (Fig. 5**a**). These numbers were much smaller than previous studies, e.g., 34 Mg in 2016 by Liu et al. (2020b). Interestingly, we found that the trapped Hg fluxes were decoupled with the sedimentation fluxes (MWR 2016; MWR 2018; MWR 2021). Specifically, the settled sediment (and Hg) fluxes in 2016, 2018, and 2021 were 33.4 million tons (34 Mg Hg), 104.2 million tons (21.74 Mg Hg), and 71.6 million tons (9.69 Mg Hg), respectively. The settled sediment fluxes were much higher in 2018 than in 2016 and 2021, which could be related to the grain size of sediment and the erosion events at upstream (Yang et al., 2022). However, the Hg concentrations in sediments were much higher in 2016 than in 2018 and 2021.

We found that some sub-watersheds (Mainstream-up1–3) were shifted from a sink of Hg to a source in 2018 and 2021 (Fig. 2). As discussed above, the reduction of Hg emissions led to a decrease of its presence in the mainstream of the Yangtze River. However, the disturbance of settled Hg could cause re-contamination in rivers due to changes in sediment processes (Gao et al., 2017; Gao et al., 2018). The Hg fluxes in mainstream-up reaches 1–3 increased by 3.34, 5.29, and 3.9 Mg from 2018 to 2021, respectively. Similarly, the Hg fluxes in tributaries could be also increased by the resuspension of settled Hg in sediments. Prior research highlighted the obstructive impacts of TGD with less attention to the Hg reservoir within TGD (Liu et al., 2020b). In total, 2.48 billion tons of sediments were settled in the TGD reservoir till 2021, which was ten times more than the sediments that were transported to the ocean in 2021. Based on the SPM THg concentrations found in this study (50–100 ng/g), we estimated that there was a total of 124–248 Mg THg settled in TGD reservoirs. The TGD could thus be an important source of Hg in the Yangtze River watershed.

4. Conclusion

In this study, we analyzed the Hg content in the SPM of the Yangtze River and calculated the Hg flux and budgets to the East China Sea in 2018 and 2021. The highest concentrations were found near high-emission cities and tributaries. The Hg flux to sea was relatively lower in 2018 and 2021 than in 2016, likely reflecting the changes in vegetation cover and erosion control management. The Three Georges Dam was found as a major sink of Hg in the Yangtze River, and could represent a potential emission source. The Hg fluxes are apparently correlated with industrial emissions, but increased emissions from agricultural activities should also be noted. We also found no correlation between Hg and organic carbon and nitrogen compounds, indicating different sources or controlling mechanisms. Overall, this study serves as a useful case study to identify the primary factors affecting the Hg flux in rivers, which is the key to developing riverine Hg models. It also contributes to our understanding of the factors affecting Hg flux in rivers and provides valuable data for Hg pollution control and related policymaking.

Declaration of generative ai and AI-assisted technologies in the writing process

During the preparation of this work, the author(s) used ChatGPT 3.5 in order to polish the language. After using this tool/service, the author (s) reviewed and edited the content as needed and take(s) full responsibility for the content of the publication.

Declaration of Competing Interest

All authors declared that they have no conflicts of interest to this work. We declare that we do not have any commercial or associative interest that represents a conflict of interest in connection with the work submitted.

Data availability

Data will be made available on request.

Acknowledgment

The authors thank the anonymous reviewers and editors for their constructive comments. We acknowledge the financial support from the National Natural Science Foundation of China(NNSFC) 42177349, 41776048, the Fundamental Research Funds for the Central Universities, China (0207–14380188, 0207–14380168), the "GeoX" Interdisciplinary Research Funds for Frontiers Science Center for Critical Earth Material Cycling, Nanjing University, and the Collaborative Innovation Center of Climate Change, Jiangsu Province.

Supplementary materials

Supplementary material associated with this article can be found, in the online version, at doi:10.1016/j.watres.2023.120390.

References

Akerblom, S., Meili, M., Bishop, K., 2015. Organic Matter in Rain: an Overlooked Influence on Mercury Deposition. Environ. Sci. Technol. Lett. 2 (4), 128–132. https://doi.org/10.1021/acs.estlett.5b00009.

Amos, H.M., Jacob, D.J., Kocman, D., Horowitz, H.M., Zhang, Y., Dutkiewicz, S., Horvat, M., Corbitt, E.S., Krabbenhoft, D.P., Sunderland, E.M., 2014. Global biogeochemical implications of mercury discharges from rivers and sediment burial. Environ. Sci. Technol. 48 (16), 9514–9522. https://doi.org/10.1021/es502134t.

Ananda, J., Herath, G., 2003. Soil erosion in developing countries: a socio-economic appraisal. Environ. Manage. 68 (4), 343–353. https://doi.org/10.1016/s0301-4797(03)00082-3.

Bailon, M.X., David, A.S., Park, Y., Kim, E., Hong, Y., 2018. Total mercury, methyl mercury, and heavy metal concentrations in Hyeongsan River and its tributaries in Pohang city, South Korea. Environ. Monit. Assess. 190 (5) https://doi.org/10.1007/s10661-018-6624-4.

Boening, D.W., 2000. Ecological effects, transport, and fate of mercury: a general review. ChemosphereChemosphere 40 (12), 1335–1351. https://doi.org/10.1016/S0045-6535(99)00283-0.

Buck, C.S., Hammerschmidt, C.R., Bowman, K.L., Gill, G.A., Landing, W.M., 2015. Flux of Total Mercury and Methylmercury to the Northern Gulf of Mexico from U.S. Estuaries. Environ. Sci. Technol. 49 (24), 13992–13999. https://doi.org/10.1021/acs.est.5b03538.

Chen, J., Cao, X., Peng, S., Ren, H.R., 2017. Analysis and Applications of GlobeLand30: a Review. ISPRS Int. J. Geoinf. 6 (8) https://doi.org/10.3390/ijgi6080230.

Cranston, R.E., Buckley, D.E., 2002. Mercury pathways in a river and estuary. Environ. Sci. Technol. 6 (3), 274–278. https://doi.org/10.1021/es60062a007.

Creaser, E., Smith, J., Thomson, A., 2019. Perspectives of solid waste management in rural Cambodia. J. Humanit. Eng. 6 (2) https://doi.org/10.36479/jhe.v6i2.125.

Dadson, S.J., Hovius, N., Chen, H., Dade, W.B., Hsieh, M.- L., Willett, S.D., Hu, J.- C., Horng, M.- J., Chen, M.- C., Stark, C.P., Lague, D., Lin, J.- C., 2003. Links between erosion, runoff variability and seismicity in the Taiwan orogen. NatureNature 426 (6967), 648–651. https://doi.org/10.1038/nature02150.

Devai, I., Delaune, R.D., Devai, G., Aradi, C., Gori, S., Nagy, A.S., Talas, Z., 2007. Characterization of mercury and other heavy metals in sediment of an ecological important backwater area of River Tisza (Hungary). J. Environ. Sci. Health Part a-Toxic/Hazardous Subs. Environ. Eng. 42 (7), 859–864. https://doi.org/10.1080/10934520701373141.

Ding, Y., Peng, S., 2020. Spatiotemporal Trends and Attribution of Drought across China from 1901 to 2100. Sustainability 12 (2), 477. https://doi.org/10.3390/su12020477.

Dirbaba, N.B., Yan, X., Wu, H., Colebrooke, L.L., Wang, J., 2018. Occurrences and ecotoxicological risk assessment of heavy metals in surface sediments from Awash River Basin, Ethiopia. Water (Switzerland) 10 (5). https://doi.org/10.3390/w10050535.

Driscoll, C.T., Blette, V., Yan, C., Schofield, C.L., Munson, R., Holsapple, J., 1995. The role of dissolved organic carbon in the chemistry and bioavailability of mercury in remote Adirondack lakes. Originally published in Water Air Soil Pollut. 80, 499–508, 1995.

Driscoll, C.T., Mason, R.P., Chan, H.M., Jacob, D.J., Pirrone, N., 2013. Mercury as a global pollutant: sources, pathways, and effects. Environ. Sci. Technol. 47 (10), 4967–4983. https://doi.org/10.1021/es305071v.

Efstathiou, C.E., 2006. Estimation of type I error probability from experimental Dixon's "Q" parameter on testing for outliers within small size data sets. TalantaTalanta 69 (5), 1068–1071. https://doi.org/10.1016/j.talanta.2005.12.031.

El Kateb, H., Zhang, H., Zhang, P., Mosandl, R., 2013. Soil erosion and surface runoff on different vegetation covers and slope gradients: a field experiment in Southern Shaanxi Province, China. Catena 105, 1–10. https://doi.org/10.1016/j.catena.2012.12.012.

Feng, Y., Zheng, B.-H., Jia, H.-F., Peng, J.-Y., Zhou, X.-Y., 2021. Influence of social and economic development on water quality in Dongting Lake. Ecol. Indic. 131 https://doi.org/10.1016/j.ecolind.2021.108220.

Fornasaro, S., Morelli, G., Costagliola, P., Rimondi, V., Lattanzi, P., Fagotti, C., 2022. Total Mercury Mass Load from the Paglia–Tiber River System: the Contribution to Mediterranean Sea Hg Budget. Toxics 10 (7). https://doi.org/10.3390/toxics10070395.

Gao, J.H., Jia, J., Kettner, A.J., Xing, F., Wang, Y.P., Li, J., Bai, F., Zou, X., Gao, S., 2018. Reservoir-induced changes to fluvial fluxes and their downstream impacts on sedimentary processes: the Changjiang (Yangtze) River, China. Quat. Int. 493, 187–197. https://doi.org/10.1016/j.quaint.2015.03.015.

Gao, J.H., Jia, J., Sheng, H., Yu, R., Li, G.C., Wang, Y.P., Yang, Y., Zhao, Y., Li, J., Bai, F., Xie, W., Wang, A., Zou, X., Gao, S., 2017. Variations in the transport, distribution, and budget of 210Pb in sediment over the estuarine and inner shelf areas of the East China Sea due to Changjiang catchment changes. J. Geophys. Res. 122 (1), 235–247. https://doi.org/10.1002/2016jf004130.

Gao, S., Xing, Y., 2021. Analysis on bulk cargo transportation organization and ship transportation system optimization of Yangtze River. In: Fifth International Conference on Traffic Engineering and Transportation System (ICTETS 2021).

Guerra, A.J.T., Fullen, M.A., Jorge, M.d.C.O., Bezerra, J.F.R., Shokr, M.S., 2017. Slope processes, mass movement and soil erosion: a review. Pedosphere Pedosphere 27 (1), 27–41. https://doi.org/10.1016/s1002-0160(17)60294-7.

Han, D., Fu, Q., Gao, S., Zhang, X., Feng, J., Chen, X., Huang, X., Liao, H., Cheng, J., Wang, W., 2019. Investigate the impact of local iron–steel industrial emission on atmospheric mercury concentration in Yangtze River Delta, China. Environ. Sci. Pollut. Res. Int. 26 (6), 5862–5872. https://doi.org/10.1007/s11356-018-3978-7.

He, Q., Qiu, Y., Liu, H., Sun, X., Kang, L., Cao, L., Li, H., Ai, H., 2017. New insights into the impacts of suspended particulate matter on phytoplankton density in a tributary of the Three Gorges Reservoir, China. Sci. Rep. 7 (1) https://doi.org/10.1038/s41598-017-13235-0.

Hu, X., Liu, Q.Z., Fu, Q.Y., Xu, H., Shen, Y., Liu, D.G., Wang, Y., Jia, H.H., Cheng, J.P., 2021. A high-resolution typical pollution source emission inventory and pollution source changes during the COVID-19 lockdown in a megacity, China. Environ. Sci. Pollut. Res. Int. 28 (33), 45344–45352. https://doi.org/10.1007/s11356-020-11858-x.

Jun, C., Ban, Y., Li, S., 2014. Open access to Earth land-cover map. NatureNature 514 (7523). https://doi.org/10.1038/514434c, 434-434.

Kocman, D., Wilson, S., Amos, H., Telmer, K., Steenhuisen, F., Sunderland, E., Mason, R., Outridge, P., Horvat, M., 2017. Toward an Assessment of the Global Inventory of Present-Day Mercury Releases to Freshwater Environments. Int. J. Environ. Res. 14 (2), 138. https://doi.org/10.3390/ijerph14020138.

Kolka, R., Grigal, D.F., Verry, E.S., Nater, E.A., 1999. Mercury and organic carbon relationships in streams draining forested Upland/Peatland watersheds. J. Environ. Qual. 28, 766–775. https://doi.org/10.2134/JEQ1999.00472425002800030006X.

Kraemer, M.U.G., Yang, C.- H., Gutierrez, B., Wu, C.- H., Klein, B., Pigott, D.M., du Plessis, L., Faria, N.R., Li, R., Hanage, W.P., Brownstein, J.S., Layan, M., Vespignani, A., Tian, H., Dye, C., Pybus, O.G., Scarpino, S.V., 2020. The effect of human mobility and control measures on the COVID-19 epidemic in China. ScienceScience 368 (6490), 493–497. https://doi.org/10.1126/science.abb4218.

Lee, S.W., Lowry, G.V., Hsu-Kim, H., 2016. Biogeochemical transformations of mercury in solid waste landfills and pathways for release. Environ. Sci. Process Impacts 18 (2), 176–189. https://doi.org/10.1039/c5em00561b.

Li, M., Du, W., Tang, S., 2021. Assessing the impact of environmental regulation and environmental co-governance on pollution transfer: micro-evidence from China. Environ. Impact Assess. Rev. 86 https://doi.org/10.1016/j.eiar.2020.106467.

Liu, C., Chen, L., Liang, S., Li, Y., 2020a. Distribution of total mercury and methylmercury and their controlling factors in the East China Sea. Environ. Pollut. 258, 113667 https://doi.org/10.1016/j.envpol.2019.113667.

Liu, M., He, Y., Baumann, Z., Zhang, Q., Jing, X., Mason, R.P., Xie, H., Shen, H., Chen, L., Zhang, W., Zhang, Q., Wang, X., 2020b. The impact of the Three Gorges Dam on the fate of metal contaminants across the river-ocean continuum. Water Res. 185, 116295 https://doi.org/10.1016/j.watres.2020.116295.

Liu, M., Xie, H., He, Y., Zhang, Q., Sun, X., Yu, C., Chen, L., Zhang, W., Zhang, Q., Wang, X., 2019. Sources and transport of methylmercury in the Yangtze River and the impact of the Three Gorges Dam. Water Res. 166, 115042 https://doi.org/10.1016/j.watres.2019.115042.

Liu, M., Zhang, Q., Yu, C., Yuan, L., He, Y., Xiao, W., Zhang, H., Guo, J., Zhang, W., Li, Y., Zhang, Q., Chen, L., Wang, X., 2021. Observation-Based Mercury Export from Rivers to Coastal Oceans in East Asia. Environ. Sci. Technol. 55 (20), 14269–14280. https://doi.org/10.1021/acs.est.1c03755.

Liu, R.P., Xu, Y.N., He, F., Zhang, J.H., Chen, H.Q., Ke, H.L., Qiao, G., Xu, D.Y., Zhao, A. N., 2012. Environmental impact by heavy-metal dispersion from the fine sediments of the Shuangqiao River, Xiaoqinling gold area, China. In: 1st International Conference on Energy and Environmental Protection (ICEEP 2012), Conference. https://doi.org/10.4028/www.scientific.net/AMR.518-523.1929Location.

Liu, X., Zhang, S., Zhang, X., Ding, G., Cruse, R.M., 2011. Soil erosion control practices in Northeast China: a mini-review. Soil Tillage Res. 117, 44–48. https://doi.org/10.1016/j.still.2011.08.005.

Lyu, J., Shi, Y., Zhang, S., Liu, S., Liu, T., Xu, X., Yang, G., Gao, J., 2023. The reservoirs gradually changed the distribution, source, and flux of particulate organic carbon within the Changjiang River catchment. J. Hydrol. (Amst) 623. https://doi.org/10.1016/j.jhydrol.2023.129808.

Ma, F., Zhang, Q., Xu, D., Hou, D., Li, F., Gu, Q., 2014. Mercury removal from contaminated soil by thermal treatment with FeCl 3 at reduced temperature. ChemosphereChemosphere 117, 388–393. https://doi.org/10.1016/j.chemosphere.2014.08.012.

Ma, M., Sun, T., Du, H., Wang, D., 2018. A Two-Year Study on Mercury Fluxes from the Soil under Different Vegetation Cover in a Subtropical Region, South China. Atmosphere (Basel) 9 (1). https://doi.org/10.3390/atmos9010030.

Mao, X., Zeng, A., Hu, T., Zhou, J., Xing, Y., Liu, S., 2013. Co-control of Local Air Pollutants and CO2 in the Chinese Iron and Steel Industry. Environ. Sci. Technol. 47 (21), 12002–12010. https://doi.org/10.1021/es4021316.

Mulvaney, K.M., Selin, N.E., Giang, A., Muntean, M., Li, C.-T., Zhang, D., Angot, H., Thackray, C.P., Karplus, V.J., 2020. Mercury benefits of climate policy in China: addressing the paris agreement and the minamata convention simultaneously. Environ. Sci. Technol. 54 (3), 1326–1335. https://doi.org/10.1021/acs.est.9b06741.

Muntean, M., Janssens-Maenhout, G., Song, S.J., Giang, A., Selin, N.E., Zhong, H., Zhao, Y., Olivier, J.G.J., Guizzardi, D., Crippa, M., Schaaf, E., Dentener, F., 2018. Evaluating EDGARv4.tox2 speciated mercury emissions ex-post scenarios and their impacts on modelled global and regional wet deposition patterns. Atmos. Environ. 184, 56–68. https://doi.org/10.1016/j.atmosenv.2018.04.017.

MWR, 2016. China River Sediment Bulletin. Ministry of Water Resources (MWR), Beijing, China.

MWR, 2018. China River Sediment Bulletin. Ministry of Water Resources (MWR), Beijing, China.

MWR, 2021. China River Sediment Bulletin. Ministry of Water Resources (MWR), Beijing, China.

Noh, S., Choi, M., Kim, E., Dan, N.P., Thanh, B.X., Ha, N.T.V., Sthiannopkao, S., Han, S., 2013. Influence of salinity intrusion on the speciation and partitioning of mercury in the Mekong River Delta. Geochim. Cosmochim. Acta 106, 379–390. https://doi.org/10.1016/j.gca.2012.12.018.

Owen, J.J., Amundson, R., Dietrich, W.E., Nishiizumi, K., Sutter, B., Chong, G., 2011. The sensitivity of hillslope bedrock erosion to precipitation. Earth Surf. Processes Landforms 36 (1), 117–135. https://doi.org/10.1002/esp.2083.

Pacyna, E.G., Pacyna, J.M., Steenhuisen, F., Wilson, S., 2006. Global anthropogenic mercury emission inventory for 2000. Atmos. Environ. 40 (22), 4048–4063. https://doi.org/10.1016/j.atmosenv.2006.03.041.

Pang, Q., Gu, J., Wang, H., Zhang, Y., 2022. Global health impact of atmospheric mercury emissions from artisanal and small-scale gold mining. iScience 25 (9). https://doi.org/10.1016/j.isci.2022.104881.

Pavoni, E., Petranich, E., Signore, S., Fontolan, G., Bezzi, A., Covelli, S., 2023. Fluxes of settling sediment particles and associated mercury in a coastal environment contaminated by past mining (Gulf of Trieste, northern Adriatic Sea). J. Soils Sediments. https://doi.org/10.1007/s11368-023-03451-9.

Pazi, I., 2011. Assessment of heavy metal contamination in Candarli Gulf sediment, Eastern Aegean Sea. Environ. Monit. Assess. 174 (1–4), 199–208. https://doi.org/10.1007/s10661-010-1450-3.

Peng, D., Chen, M., Su, X., Liu, C., Zhang, Z., Middleton, B.A., Lei, T., 2023. Mercury accumulation potential of aquatic plant species in West Dongting Lake, China. Environ. Pollut. 324, 121313 https://doi.org/10.1016/j.envpol.2023.121313.

Peng, D., Liu, Z., Su, X., Xiao, Y., Wang, Y., Middleton, B.A., Lei, T., 2020. Spatial distribution of heavy metals in the West Dongting Lake floodplain, China. Environ. Sci. Process Impacts 22 (5), 1256–1265. https://doi.org/10.1039/c9em00536f.

Peng, S., Ding, Y., Liu, W., Li, Z., 2019. 1 km monthly temperature and precipitation dataset for China from 1901 to 2017. Earth System Sci. Data 11 (4), 1931–1946. https://doi.org/10.5194/essd-11-1931-2019.

Peng, Y.M., Wu, P.P., Schartup, A.T., Zhang, Y.X., 2021. Plastic waste release caused by COVID-19 and its fate in the global ocean. Proc. Natl. Acad. Sci. U.S.A. 118 (47) https://doi.org/10.1073/pnas.2111530118.

Protano, C., Zinnà, L., Giampaoli, S., Spica, V.R., Chiavarini, S., Vitali, M., 2014. Heavy metal pollution and potential ecological risks in rivers: a case study from Southern Italy. Bull. Environ. Contam. Toxicol. 92 (1), 75–80. https://doi.org/10.1007/s00128-013-1150-0.

Ramalhosa, E., Pereira, E., Vale, C., Válega, M., Monterroso, P., Duarte, A.C., 2005. Mercury distribution in Douro estuary (Portugal). Mar. Pollut. Bull. 50 (11), 1218–1222. https://doi.org/10.1016/j.marpolbul.2005.04.020.

Sangkham, S., 2020. Face mask and medical waste disposal during the novel COVID-19 pandemic in Asia. Case Stud. Chem. Environ. Eng. 2 https://doi.org/10.1016/j.cscee.2020.100052.

Schuster, P.F., Striegl, R.G., Aiken, G.R., Krabbenhoft, D.P., Dewild, J.F., Butler, K., Kamark, B., Dornblaser, M., 2011. Mercury Export from the Yukon River Basin and Potential Response to a Changing Climate. Environ. Sci. Technol. 45 (21), 9262–9267. https://doi.org/10.1021/es202068b.

Selin, N.E., Jacob, D.J., Yantosca, R.M., Strode, S., Jaeglé, L., Sunderland, E.M., 2008. Global 3-D land-ocean-atmosphere model for mercury: present-day versus preindustrial cycles and anthropogenic enrichment factors for deposition. Global Biogeochem. Cycles 22 (2). https://doi.org/10.1029/2007 gb003040 n/a-n/a.

Shangguan, W., Dai, Y., Liu, B., Zhu, A., Duan, Q., Wu, L., Ji, D., Ye, A., Yuan, H., Zhang, Q., Chen, D., Chen, M., Chu, J., Dou, Y., Guo, J., Li, H., Li, J., Liang, L., Liang, X., Liu, H., Liu, S., Miao, C., Zhang, Y., 2013. A China data set of soil properties for land surface modeling. J. Adv. Model. Earth Syst. 5 (2), 212–224. https://doi.org/10.1002/jame.20026.

Shao, S., Li, B., Fan, M., Yang, L., 2021. How does labor transfer affect environmental pollution in rural China? Evidence from a survey. Energy Econ. 102 https://doi.org/10.1016/j.eneco.2021.105515.

Shen, H., Tao, S., Chen, Y., Ciais, P., Guneralp, B., Ru, M., Zhong, Q., Yun, X., Zhu, X., Huang, T., Tao, W., Chen, Y., Li, B., Wang, X., Liu, W., Liu, J., Zhao, S., 2017. Urbanization-induced population migration has reduced ambient PM(2.5) concentrations in China. Sci. Adv. 3 (7), e1700300 https://doi.org/10.1126/sciadv.1700300.

Shen, L., Zhao, T., Wang, H., Liu, J., Bai, Y., Kong, S., Zheng, H., Zhu, Y., Shu, Z., 2021. Importance of meteorology in air pollution events during the city lockdown for COVID-19 in Hubei Province, Central China. Sci. Total Environ. 754 https://doi.org/10.1016/j.scitotenv.2020.142227.

Sun, G., Li, Z., Bi, X., Chen, Y., Lu, S., Yuan, X., 2013. Distribution, sources and health risk assessment of mercury in kindergarten dust. Atmos. Environ. 73, 169–176. https://doi.org/10.1016/j.atmosenv.2013.03.017.

Wang, C., Zhang, C., Wang, Y., Jia, G., Wang, Y., Zhu, C., Yu, Q., Zou, X., 2022. Anthropogenic perturbations to the fate of terrestrial organic matter in a river-dominated marginal sea. Geochim. Cosmochim. Acta 333, 242–262. https://doi.org/10.1016/j.gca.2022.07.012.

Wang, X., Lin, C.-J., Yuan, W., Sommar, J., Zhu, W., Feng, X., 2016. Emission-dominated gas exchange of elemental mercury vapor over natural surfaces in China. Atmos. Chem. Phys. 16 (17), 11125–11143. https://doi.org/10.5194/acp-16-11125-2016.

XU, X., 2021. Impacts of China's Ten-Year Fishing Ban Policy on the Lower Reaches of the Yangtze River Basin. Imperial College London. MSc.

XU Xinliang, L.L., 2014. 1 km grid GDP data of China (2005, 2010). Acta Geogr. Sin. 69 (s1), 45–48. https://doi.org/10.11821/dlxb2014S007.

Yang, S.L., Milliman, J.D., Xu, K.H., Deng, B., Zhang, X.Y., Luo, X.X., 2014. Downstream sedimentary and geomorphic impacts of the Three Gorges Dam on the Yangtze River. Earth Sci. Rev. 138, 469–486. https://doi.org/10.1016/j.earscirev.2014.07.006.

Yang, Y., Zheng, J., Zhu, L., Zhang, H., Wang, J., 2022. Influence of the Three Gorges Dam on the transport and sorting of coarse and fine sediments downstream of the dam. J. Hydrol. (Amst) 615. https://doi.org/10.1016/j.jhydrol.2022.128654.

Yi, Y., Yang, Z., Zhang, S., 2011. Ecological risk assessment of heavy metals in sediment and human health risk assessment of heavy metals in fishes in the middle and lower reaches of the Yangtze River basin. Environ. Pollut. 159 (10), 2575–2585. https://doi.org/10.1016/j.envpol.2011.06.011.

Yin, S., Gao, G., Ran, L., Li, D., Lu, X., Fu, B., 2023. Extreme streamflow and sediment load changes in the Yellow River Basin: impacts of climate change and human activities. J. Hydrol. (Amst) 619. https://doi.org/10.1016/j.jhydrol.2023.129372.

Zhang, Y., Wang, M., Huang, B., Akhtar, M.S., Hu, W., Xie, E., 2018. Soil mercury accumulation, spatial distribution and its source identification in an industrial area of the Yangtze Delta, China. Ecotoxicol. Environ. Saf. 163, 230–237. https://doi.org/10.1016/j.ecoenv.2018.07.055.

Zolkos, S., Krabbenhoft, D.P., Suslova, A., Tank, S.E., McClelland, J.W., Spencer, R.G.M., Shiklomanov, A., Zhulidov, A.V., Gurtovaya, T., Zimov, N., Zimov, S., Mutter, E.A., Kutny, L., Amos, E., Holmes, R.M., 2020. Mercury Export from Arctic Great Rivers. Environ. Sci. Technol. 54 (7), 4140–4148. https://doi.org/10.1021/acs.est.9b07145.